

# Boron neutron capture therapy demonstrated in mice bearing EMT6 tumors following selective delivery of boron by rationally designed liposomes

Peter J. Kueffer, Charles A. Maitz, Aslam A. Khan, Seth A. Schuster, Natalia I. Shlyakhtina, Satish S. Jalisatgi, John D. Brockman, David W. Nigg<sup>1</sup>, and M. Frederick Hawthorne<sup>2</sup>

International Institute of Nano and Molecular Medicine, University of Missouri, Columbia, MO 65211

Contributed by M. Frederick Hawthorne, February 27, 2013 (sent for review January 22, 2013)

The application of boron neutron capture therapy (BNCT) following liposomal delivery of a <sup>10</sup>B-enriched polyhedral borane and a carborane against mouse mammary adenocarcinoma solid tumors was investigated. Unilamellar liposomes with a mean diameter of 134 nm or less, composed of an equimolar mixture of cholesterol and 1,2-distearoyl-*sn*-glycero-3-phosphocholine and incorporating Na<sub>3</sub>[1-(2'-B<sub>10</sub>H<sub>9</sub>)-2-NH<sub>3</sub>B<sub>10</sub>H<sub>8</sub>] in the aqueous interior and K[nido-7-CH<sub>3</sub>(CH<sub>2</sub>)<sub>15</sub>-7,8-C<sub>2</sub>B<sub>9</sub>H<sub>11</sub>] in the bilayer, were injected into the tail veins of female BALB/c mice bearing right flank EMT6 tumors. Biodistribution studies indicated that two identical injections given 24 h apart resulted in tumor boron levels exceeding 67 μg/g tumor at 54 h—with tumor/blood boron ratios being greatest at 96 h (5.68:1; 43 μg boron/g tumor)—following the initial injection. For BNCT experiments, tumor-bearing mice were irradiated 54 h after the initial injection for 30 min with thermal neutrons, resulting in a total fluence of 1.6 × 10<sup>12</sup> neutrons per cm<sup>2</sup> (±7%). Significant suppression of tumor growth was observed in mice given BNCT vs. control mice (only 424% increase in tumor volume at 14 d post irradiation vs. 1551% in untreated controls). In a separate experiment in which mice were given a second injection/irradiation treatment 7 d after the first, the tumor growth was vastly diminished (186% tumor volume increase at 14 d). A similar response was obtained for mice irradiated for 60 min (169% increase at 14 d), suggesting that neutron fluence was the limiting factor controlling BNCT efficacy in this study.

oncology | radiation | cancer | nanoparticles

**B**oron neutron capture therapy (BNCT) is a binary treatment modality for cancer involving the selective accumulation of chemical agents containing the isotope <sup>10</sup>B in cancer cells followed by irradiation with thermal neutrons. Capture of a thermal neutron by a <sup>10</sup>B nucleus initiates a nuclear reaction in which decay of an excited <sup>11</sup>B nucleus produces a high linear energy transfer α-particle and lithium nucleus. Because of the short trajectory of these heavy particles (5–9 μm; approximately one cell diameter), radiation damage is limited to those cells containing <sup>10</sup>B. Thus, if <sup>10</sup>B agents can be selectively targeted to tumor cells, side effects typically associated with ionizing radiation can be avoided.

For BNCT to be successful in the treatment of cancer, the following criteria must be completely addressed: (i) preferential or selective uptake of <sup>10</sup>B-containing agent(s) by tumor tissue, relative to normal tissue, at concentrations sufficiently high to deliver a therapeutic dose of <sup>10</sup>B atoms (≥20 μg <sup>10</sup>B per gram of tumor tissue or 10<sup>9</sup> atoms <sup>10</sup>B per cell); (ii) retention of <sup>10</sup>B in tumor tissue with rapid clearance from blood and normal tissues; and (iii) low systemic toxicity of all <sup>10</sup>B delivery agents (1–7). Practically speaking, the <sup>10</sup>B agents used should not be excessively difficult or cost-prohibitive to prepare, and their synthesis should occur in high yield from readily available starting materials and be amenable to scale up.

Historically, efforts to develop agents useful for BNCT have been too narrow, focusing almost exclusively on the treatment of

the aggressive and deadly brain tumor glioblastoma multiforme (GBM) (7–10). In identifying potential agents for neutron capture, emphasis was placed on screening candidate molecules for this purpose rather than fully considering their rational design. In the case of GBM, agent choice was based primarily on whether specific challenges could be overcome, for example, achieving high tumor/blood boron ratios with secondary consideration given to high tumor/blood ratios.

At present, three compounds are approved for human trials, namely boronophenylalanine, sodium mercaptoundecahydro-*closo*-dodecaborate, and disodium-decahydro-*closo*-decaborate. Use of these agents for BNCT of GBM, melanoma, and head and neck cancers has met with limited success; treatments are largely palliative or last-line and are therefore only marginally more effective than conventional external-beam radiation therapy in increasing survival times (10–15). With BNCT research having been so limited in scope, many agents that might have been highly effective against other more treatable types of cancer were never evaluated beyond preliminary studies. Only in the past 20 y has BNCT research begun to address other cancers. Even so, the vast majority of this work on potential new <sup>10</sup>B agents has not progressed beyond small animal biodistribution studies, and most have failed to meet all the requirements for successful BNCT (4–7).

To fully establish a practical system of BNCT for cancer, the fundamental chemistry of the boron-containing compounds being used and the means of conveying those compounds to the tumor must be considered. Liposomes are especially appealing as boron delivery vehicles because they will passively accumulate in most tumors by means of the enhanced permeability and retention effect (16, 17). By using this tumor targeting property, our laboratory successfully used unilamellar liposomes in vivo for delivery of anionic polyhedral boranes to murine EMT6 mammary adenocarcinoma tumors (18). In our subsequent in vivo studies, we demonstrated selective delivery of boron-rich liposomes containing hydrophilic polyhedral borane anions encapsulated in the aqueous core, lipophilic carboranes embedded in the bilayer membrane, or both (7, 19) (Fig. 1).

The polyhedral boranes [*closo*-B<sub>10</sub>H<sub>10</sub>]<sup>2-</sup> and [*closo*-B<sub>12</sub>H<sub>12</sub>]<sup>2-</sup> possess many unique properties that make them excellent scaffolds upon which to construct BNCT agents. In addition to their high boron content, they exhibit high water solubility and extremely low toxicity (20). The dimer [*trans*-B<sub>20</sub>H<sub>18</sub>]<sup>2-</sup>, a species readily

Author contributions: C.A.M., S.S.J., and M.F.H. designed research; P.J.K., C.A.M., A.A.K., S.A.S., and N.I.S. performed research; P.J.K., A.A.K., N.I.S., J.D.B., and D.W.N. contributed new reagents/analytic tools; P.J.K., C.A.M., A.A.K., S.A.S., S.S.J., and M.F.H. analyzed data; J.D.B. and D.W.N. performed neutron dosimetry; and P.J.K., C.A.M., A.A.K., S.S.J., and M.F.H. wrote the paper.

The authors declare no conflict of interest.

<sup>1</sup>Present address: Idaho National Laboratory, Idaho Falls, ID 83415.

<sup>2</sup>To whom correspondence should be addressed. E-mail: hawthornem@missouri.edu.

This article contains supporting information online at [www.pnas.org/lookup/suppl/doi:10.1073/pnas.1303437110/-DCSupplemental](http://www.pnas.org/lookup/suppl/doi:10.1073/pnas.1303437110/-DCSupplemental).

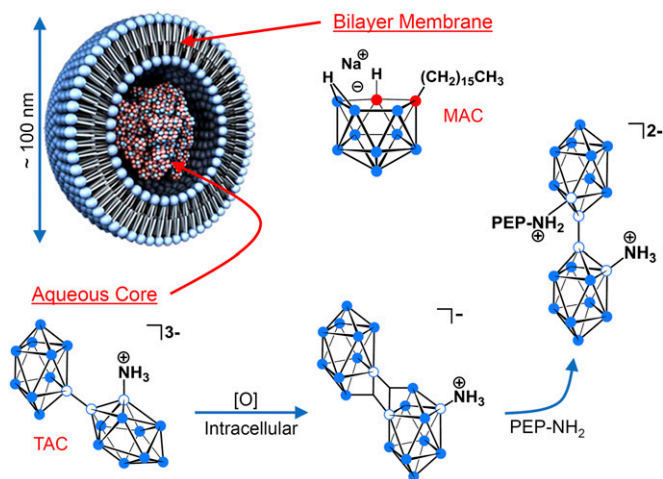


**Fig. 1.** Liposomal formulation in which the lecithin/cholesterol bilayer membrane incorporates the lipophilic boron agent MAC, acting as a complement to the hydrophilic polyhedral borane TAC, which is encapsulated in the aqueous core (filled blue circle = boron-hydrogen; empty blue circle = boron; and filled red circle = carbon). Upon release from liposomes and exposure to an oxidant, [O], in the tumor cell interior, TAC undergoes conversion to the electrophilic species  $[B_{20}H_{17}NH_3]^-$ , which possesses a pair of three-center two-electron bonds and is isoelectronic with  $[trans-B_{20}H_{18}]^{2-}$ . An encounter of  $[B_{20}H_{17}NH_3]^-$  with an intracellular protein containing a peptide (PEP) that bears a nucleophile (i.e.,  $NH_2$ ) will result in covalent bond formation, attaching TAC to the peptide. The isomer shown is the more clearly indicated product of nucleophilic addition to  $[B_{20}H_{17}NH_3]^-$  (26).

synthesized from  $[closo-B_{10}H_{10}]^{2-}$ , is of particular utility. When it is converted to an ammonio derivative,  $Na_3[1-(2'-B_{10}H_9)-2-NH_3B_{10}H_8]$  (TAC), liposomal delivery provides notably large, therapeutic concentrations of boron in the tumor, with long periods of retention (21). Evidence suggests that the persistence of TAC in the tumor is a result of covalent bond formation with nucleophiles present on endogenous intracellular proteins (21–27) (Fig. 1). Nucleophilic attack presumably occurs following conversion of TAC to the reactive species  $[B_{20}H_{17}NH_3]^-$  (25–27), which is readily produced in oxidizing environments like those often possessed by tumor cell interiors (28, 29). Experiments have provided spectroscopic and crystallographic confirmation that binding occurs on the unsubstituted boron cage (26), although other isomers are possible, and all would serve to prolong confinement of TAC to the intracellular medium.

An inherent drawback in the preparation of small unilamellar liposomes is that only a small percentage of the total solution containing a BNCT agent is encapsulated, limiting the amount of boron that can be delivered to tumors via the liposomal interior alone (21). To ameliorate this issue, our laboratory devised a complementary lipophilic agent,  $K[nido-7-CH_3(CH_2)_{15}-7,8-C_2B_9H_{11}]$  (MAC), which is stably incorporated into the liposome bilayer (30). We demonstrated that inclusion of this amphiphilic *nido*-carborane in the bilayer yielded selective accumulation of high levels of boron in tumors alone or in combination with encapsulated borane salts (19, 30). Furthermore, MAC increases the efficiency of overall liposome uptake by cells. This characteristic arises from the negative surface charge MAC imparts to the liposomes, a property that has been demonstrated to enhance cellular adhesion, leading to greater internalization via clathrin-mediated endocytosis (31–34).

No systemic toxicity or side effects have been observed in any biodistribution studies performed with the use of TAC and MAC (35). It is also noteworthy that both compounds are readily attainable by straightforward, high-yield, scalable processes, and they are stable for long periods of time before administration.

Hence, the boron agents and delivery system we have developed fulfill all the requirements for successful BNCT. Our continued progress was impeded only by the lack of access to an appropriate neutron source with which to perform therapeutic efficacy trials. The construction of a thermal neutron beam line at the University of Missouri Research Reactor has now permitted us to conduct these critical investigations (36).

Reported here are results of BNCT applied to localized EMT6 solid flank tumors in BALB/c mice injected with liposomes carrying the polyhedral borane TAC and the *nido*-carborane MAC. Substantial inhibition of tumor growth was observed in mice receiving BNCT compared with untreated controls and to mice receiving thermal neutron irradiation only. Biodistribution studies were performed to optimize the liposome injection protocol and to confirm the selective accumulation and retention of therapeutic amounts of  $^{10}B$  in tumors before irradiation.

## Results and Discussion

**Biodistribution Studies.** Experiments were performed to monitor the distribution of boron in tumor, blood, and normal tissues over time to identify the optimal injection protocol for delivery of boron to tumor tissue. Our first procedure consisted of a single 200- $\mu$ L tail-vein injection of unilamellar liposomes incorporating TAC and MAC compounds [volume-weighted mean vesicle diameter ( $m_v$ ), 122 nm], with injected dose of boron being 342  $\mu$ g ( $\sim 17 \mu$ g  $^{10}B$  per gram of body mass). Sufficient tissues were collected and analyzed to confirm our previous biodistribution time-course results using this injection protocol in EMT6 tumor-bearing mice (30). The present biodistribution results are shown in Fig. 2A. Tumor boron levels were sufficient for BNCT at 18 h and 30 h post injection (28.0 and 27.2  $\mu$ g  $^{10}B$  per gram of tumor, respectively); however, the highest tumor/blood boron ratio (2.76:1) was not achieved until 48 h, when the boron concentration was only 18.1  $\mu$ g  $^{10}B$  per gram tumor. Therefore, a “double-injection” protocol was investigated.

A double-injection protocol was tested in which two 200- $\mu$ L injections of liposomes ( $m_v$  of 106 nm; 371  $\mu$ g of boron per injection, 18.6  $\mu$ g  $^{10}B$  per gram body mass) were administered 24 h apart. To examine the full biological impact of a double injection, boron content was assessed in multiple different tissues over a prolonged time interval. The resulting biodistribution of boron in murine tissues over time is shown in Fig. 2B. With the double-injection protocol, higher peak boron concentrations were obtained in all tissues compared with a single injection because clearance from the first injection was not complete by 24 h (Fig. 2A). Delayed clearance of boron from the tumors caused boron levels to peak in tumor tissue 54 h after the first injection. Concentrations in liver and spleen also peaked at 54 h; by contrast, boron levels in the blood were decreasing by 48 h. At 54 h, boron concentration in the tumors was 67.8  $\mu$ g  $^{10}B$  per gram tumor, and the tumor/blood boron ratio was 1.88:1. As clearance of boron from blood proceeded more rapidly than loss from tumors, the tumor/blood ratio continued to increase after 54 h. At 72 h, the ratio was 2.76:1, and, by 96 h, it had reached 5.66:1. The tumor boron concentrations at 72 h and 96 h were 57.4  $\mu$ g  $^{10}B$  per gram tumor and 43.0  $\mu$ g  $^{10}B$  per gram tumor, respectively.

A notable feature of the double-injection scheme is the wide window of time available for neutron irradiation—the concentration of boron in the tumors remains well within the therapeutic range for at least 96 h after the initial injection while tumor/blood boron ratios continue to increase. Considering these results, the double-injection protocol was ultimately adopted for irradiation studies. In addition, the 54-h time point was chosen as most optimal for irradiation, with the initial assumption having been that a greater tumor boron concentration was the most influential factor in BNCT efficacy.

**Irradiation Studies.** Dose-escalation studies were conducted by varying the duration of neutron irradiation. Three data sets were

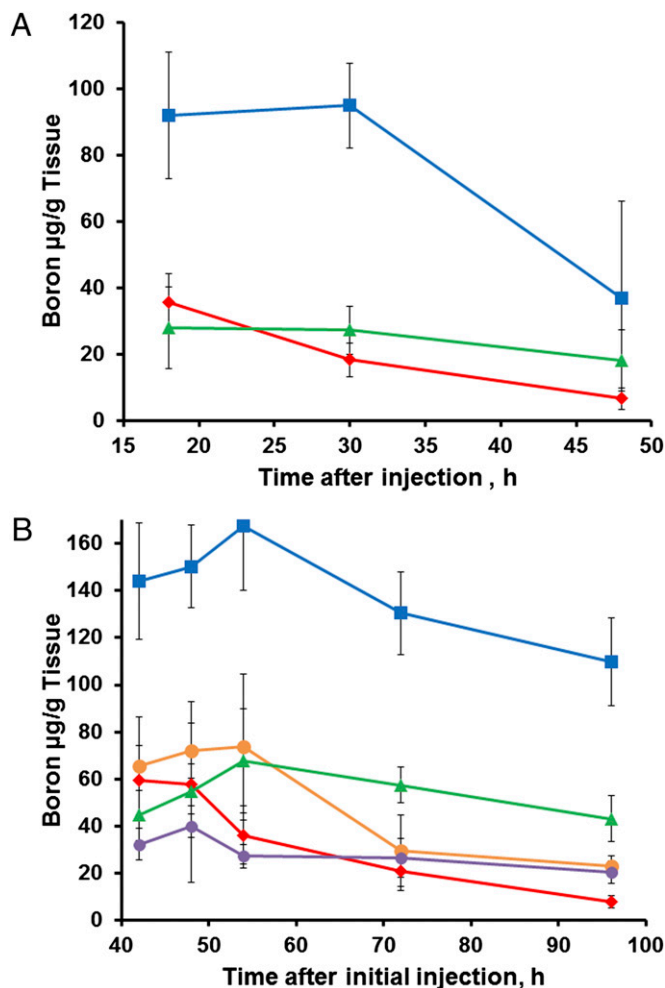


**Fig. 2.** Distribution of boron in mouse tissues over time following TAC/MAC liposomal injections (red diamond = blood; blue square = liver; orange circle = spleen; purple circle = kidney; green triangle = tumor). (A) Single injection of TAC/MAC liposomal suspension (combination of two studies with injected doses of 345 or 340  $\mu\text{g}$  of boron). (B) Double injection of TAC/MAC liposomal suspension (two single injections performed 24 h apart totaling an injected dose of 742  $\mu\text{g}$  of boron). Data points are means and error bars depict  $\pm$  SD. Sample size for each time point varied but was never less than  $n = 4$  (SI Text).

collected, including a single irradiation study of 30 min duration, a double irradiation study whereby a 30-min irradiation was repeated after 7 d (following another double injection), and a single irradiation of 60 min duration. In the 30-min single-irradiation study, liposomes ( $m_w$ , 130 nm) containing  $^{10}\text{B}$ -enriched TAC and MAC were injected into the tail vein of 12 treatment mice following the double-injection protocol at a dose of 342  $\mu\text{g}$  boron (17.1  $\mu\text{g}$   $^{10}\text{B}$  per gram body mass) per injection. At 54 h after the initial injection, the mice were irradiated for 30 min, resulting in a total fluence of  $1.6 \times 10^{12}$  neutrons/cm<sup>2</sup>. Fourteen “neutron-only” mice that received no injections of any kind were irradiated under the same conditions. Both groups of mice were compared with an untreated control group of 23 mice that received neither injections nor irradiation.

Fig. 3A demonstrates that, in mice given a single 30-min BNCT treatment, tumor growth was significantly slower compared with untreated controls. Data for the neutron only group were omitted from the plot for clarity but are available in SI Text. The rapid rate of tumor enlargement and concomitant decline in the health status of the nontreated control mice prevented assessments of tumor volume beyond 14 d post irradiation. By 14 d, tumor

volume in the control mice had increased by 1,551%, whereas the volume in mice given BNCT had increased by only 424%. The tumor volume increase in neutron-only mice was 737%, suggesting some inhibitory effect from irradiation alone. Therefore, further evaluation by Kaplan–Meier time-to-event analysis (37) was conducted (Fig. 4). The median time for tumors to reach a volume of 500 mm<sup>3</sup> in mice given BNCT was 22 d, statistically significant at the 5% level compared with 14 d for mice receiving neutron irradiation only ( $P < 0.002$ ) or 12 d for the untreated control mice ( $P < 0.001$ ). Comparison of the median tumor growth times of neutron-only mice with untreated controls was significant at the 5% level but not at the 1% level ( $P = 0.012$ ).

In the next study, the effect of two identical rounds of BNCT was examined in an experiment in which four mice were administered a second treatment 7 d after the first. Mice were given another double injection by using the same liposome suspension described earlier, and the mice were again irradiated for 30 min at 54 h after the initial injection. Fig. 3B demonstrates that retreatment had an additional impact on tumor growth. At 14 d post irradiation, tumor volume had increased only by 186%; even by 21 d, volume increase was only 297%.

To determine whether neutrons were a limiting factor in our BNCT treatment, the effect of a longer duration of neutron irradiation on tumor growth was examined in the final study. Four mice were given a double injection of liposomes ( $m_w$ , 113 nm; injected dose, 351  $\mu\text{g}$  of boron per injection; 17.6  $\mu\text{g}$   $^{10}\text{B}$  per gram body mass) and, at 54 h after the initial injection, mice were irradiated for 30 min. Immediately following the irradiation, mice were allowed to recover from anesthesia for 15 min before being anesthetized again and irradiated for another 30 min. This procedure effectively doubled the amount of time the mice were irradiated at the 54-h time point of the double-injection treatment protocol. Although the data set is limited as a result of excessive difficulty in recovering animals from the second round of anesthesia, the results show that doubling the irradiation time leads to additional suppression of tumor growth (Fig. 3C). Tumor volume increase at 14 d was 169%, and, at 21 d, was 233%, a reduction comparable to that obtained when two rounds of BNCT were administered 1 wk apart (Fig. 3B).

None of the mice in the experiments performed exhibited any apparent deleterious effects from BNCT. No toxic effects from liposomal injections were detected, and no radiation side effects were observed, even in those mice exposed to the neutron beam for 1 h. Although the inability to identify any effects on the skin or in other organs precluded calculation of a relative biological effectiveness for the neutron beam or a compound biological effectiveness for the boronated liposomes, the lack of observable detrimental effects is encouraging because it allows for the possibility of further boron and neutron dose escalation. Dose-limiting side effects have been encountered in several human and animal trials of BNCT that could at least in part be attributed to the relatively high relative biological effectiveness of the background epidermal, fast neutron, and  $\gamma$ -spectral components of the neutron beams (38). The thermal neutron beam constructed for our BNCT studies possesses minimal  $\gamma$ - and fast neutron contamination (36).

The present study had some identified limitations. First, the duration of radiation and therefore the total neutron fluence was restricted by the 30-min anesthesia limit for the mice. For BNCT to be effective, total thermal (0–0.414 eV) neutron fluence must be at least  $1 \times 10^{12}$  neutrons/cm<sup>2</sup>. A 30-min exposure to the University of Missouri Research Reactor neutron beam provides a total thermal neutron fluence of  $1.6 \times 10^{12}$  ( $\pm 7\%$ ). Although this level of neutron fluence was ostensibly sufficient, the additional tumor suppression attained in mice that received two successive 30-min irradiations suggests that neutron fluence was the primary factor restricting BNCT efficacy in this study. Given the large window of time available for neutron irradiation using the double-injection



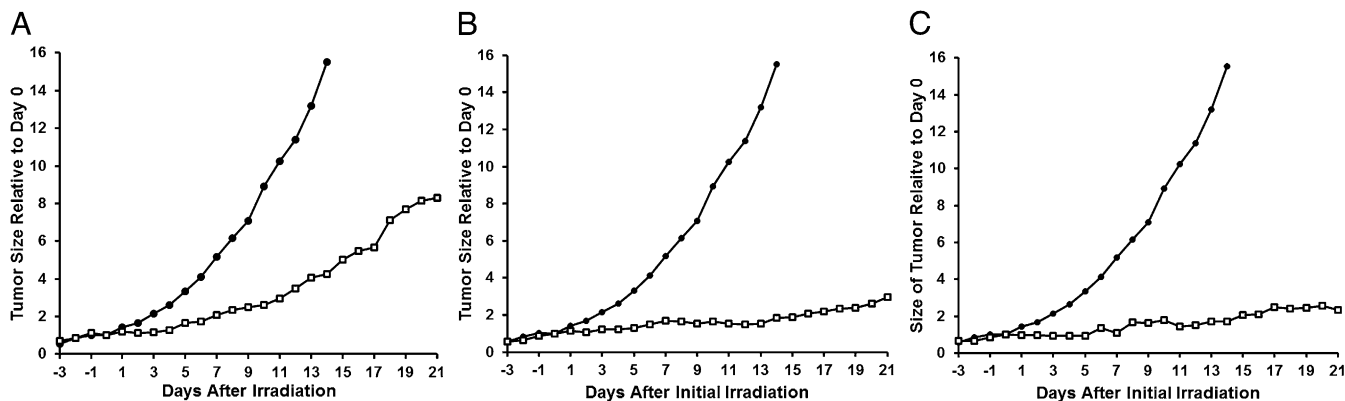


**Fig. 3.** Tumor growth curves normalized with respect to average volume at day 0 (set as the time of irradiation): ● control group; □, BNCT group. (A) Single BNCT treatment consisting of a 30-min irradiation following double injection of liposomal suspension. (B) Two single BNCT treatments (double injection of liposomal suspension, 30 min irradiation) performed 7 d apart. (C) Single BNCT treatment consisting of a 1-h irradiation following double-injection of liposomal suspension. Neutron-only data excluded for clarity and are available in *SI Text*.

protocol, a second irradiation at a safer time with regard to anesthesia (e.g., 2–6 h later) should be explored.

A second limitation was the profound effect of tumor size on total boron uptake. In the case of our tumor model, this characteristic was attributed to internal necrosis, which may exist when the tumor mass nears or exceeds 150 mg. Such necrosis has been observed in other poorly vascularized tumor interiors as they begin to outgrow their blood supply; larger tumors are therefore more likely to only retain boron agents in their peripheries (39, 40). Although this would not preclude BNCT treatment of the tumor, it would diminish the apparent boron concentration in the tumor and prevent complete eradication of any quiescent cell population.

Also, implanted flank tumors, by their very nature, may have a more limited blood supply and therefore be more susceptible to problems concerning BNCT agent delivery. Chemically induced or spontaneous tumors might be less affected by this problem and therefore more effectively controlled by BNCT alone, with results potentially equaling or surpassing those achieved with EMT6 tumors treated with cytotoxic agents (41, 42). To verify this, BNCT studies that use our liposomal formulations in a well-characterized, small animal oral mucosa tumor model (43) are nearing completion in a separate collaboration with the Division of Radiation Pathology at the National Atomic Energy Commission of Argentina.

A significant advantage of the double-injection protocol is the broad window in which neutron irradiation can be administered. The biodistribution studies showed that tumor/blood boron ratios continue to increase for 54 to 96 h after the initial injection while tumor boron concentrations remain at therapeutic levels for all time points. Ideally, the concentrations of boron in normal tissues during this time should be as low as possible to minimize collateral damage from neutron capture. Nevertheless, a high postinjection concentration of boron in liver was observed and anticipated, as liposomal clearance primarily occurs through the reticuloendothelial system. Suitable shielding and positioning of the animals during irradiation prevented any apparent damage to the liver, and no inherent hepatotoxicity of the liposomes themselves was evident.

These experiments establish proof of concept for the successful suppression of tumor growth by BNCT following delivery of therapeutic quantities of boron to tumors via liposomes carrying polyhedral boranes and carboranes. Research efforts by our group and affiliates (35) are currently directed at applying the treatment protocol reported here to other cancer types and have, in some instances, achieved complete cancer remission. Furthermore, ongoing neutron dose-escalation studies performed on the same cancer type (EMT6) by using our delivery system have demonstrated enhanced tumor control beyond the results presented in this report. Additional therapeutic agents are also being evaluated for use in the liposomal delivery system. Concurrently, alternative systems are being investigated in which the therapeutic agent is covalently combined with the delivery system to increase boron uptake, enhance stability, and even circumvent the need for  $^{10}\text{B}$ -enrichment of the boron compounds. Nanoparticles with these features are presently being designed and will offer the capability of facile surface modification to increase circulation time, apply a specific targeting mechanism, allow for additional ease of scalability, and reduce cost of therapy. Preparations are also being made for the study of the effectiveness of our BNCT regimen in larger animals such as dogs, paving the way for eventual human trials.

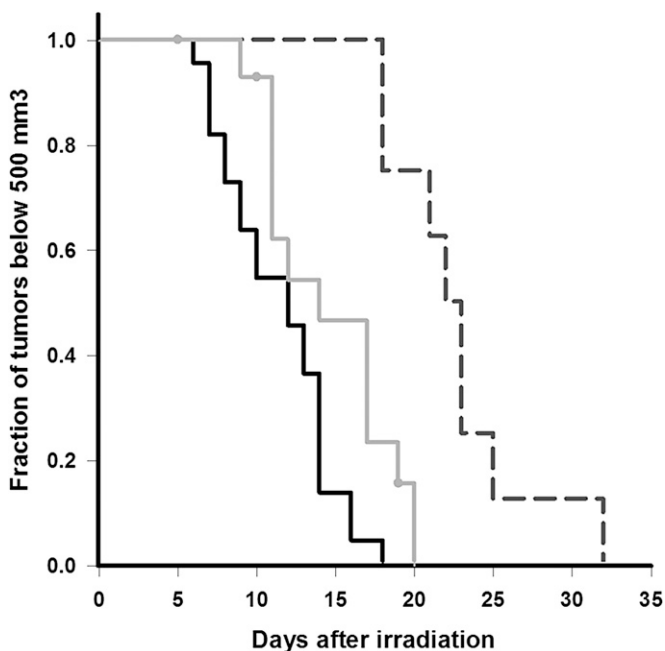


**Fig. 4.** Kaplan–Meier time-to-event curves indicating time required to reach a 500- $\text{mm}^3$  tumor volume (solid black line, control group; solid gray line, neutron only group; dashed line, BNCT group). The y axis indicates fraction of mice having not yet developed a tumor greater than 500  $\text{mm}^3$ . Time 0 indicates the day of irradiation for the BNCT and neutron-only mice; all mice were implanted with tumor cells on the same day. The median time represents the least amount of time (in days) required for 50% (0.5) of the mice to develop a tumor  $\geq 500 \text{ mm}^3$ .

## Materials and Methods

**Compounds.** Boron 10-enriched MAC and TAC were prepared under inert (argon) atmospheres by using methods previously described (21, 22, 30) and beginning from  $^{10}\text{B}$ -enriched decaborane, with the percentage of  $^{10}\text{B}$  being 95% or greater. Liposome suspensions were created by probe sonication of dried films (300 mg) comprised of 1,2-distearoyl-*sn*-glycero-3-phosphocholine (Avanti Polar Lipids), cholesterol (Aldrich), and MAC in a 1:1:0.6 molar ratio, respectively, immersed in a hypertonic wetting solution consisting of TAC (250 mM) in 6 mL water. Samples were sonicated continuously for 40 min in a water bath maintained at  $65 \pm 0.5$  °C. Excess wetting solution was separated from the liposome suspension by elution from a Sephadex G-25 (medium) column equilibrated with isotonic phosphate-buffered lactose (5 mM phosphate/9% (wt/wt) lactose, pH 7.4) or PBS solution (10 mM phosphate/2.7 mM KCl/137 mM NaCl, pH 7.4). Liposome suspensions were diluted with the appropriate buffer to a final volume of 12 mL and filtered through two sterile 0.2- $\mu\text{m}$  syringe filters into sterile serum bottles. The  $m_n$  of the liposomes ranged from 109 nm to 134 nm as determined by dynamic light scattering at 25 °C. Measurements using electrophoretic light scattering in water at 25 °C provided a  $\zeta$ -potential of the liposome suspensions of  $-76.4 \pm 1.1$  mV ( $n = 4$ ), indicating a high degree of resistance to aggregation.

**Cell Culture, Tumor Induction, and Experimental Design.** EMT6 cells were purchased from American Type Culture Collection and cultured in Weymouth medium supplemented with 10% FBS as recommended by American Type Culture Collection. Cells in log phase were dissociated by incubation with TrypLE buffer (Life Technologies) for 10 min, followed by addition of FBS-containing medium to terminate TrypLE digestion. Cells were then centrifuged at  $323 \times g$  for 8 min at room temperature using Fisher Scientific accupspin 3R centrifuge, and the cell pellets were resuspended in PBS solution. Cells were counted using a Countess Automatic Cell Counter (Life Technologies). For tumor production, EMT6 cells ( $1 \times 10^6$  cells/mouse) were inoculated into the right flank of female BALB/c mice having an average body weight of  $20 \pm 1$  g, following standard protocols (18). Animals were typically purchased in groups of 12 mice (Harlan Laboratories) for tumor inoculation and were assigned to the study groups described later contingent upon how quickly the tumors reached the target volume. All animal procedures were conducted in accordance with protocols approved by the University of Missouri Animal Care and Use Committee.

**Biodistribution Studies.** When the tumors had reached a target volume of 80 to 150  $\text{mm}^3$ , mice were administered boron-containing liposomes via lateral tail vein injection, and the distribution of boron in blood and organs was evaluated at specific intervals after injection. The injection protocol consisted of a single 200- $\mu\text{L}$  injection or two identical 200- $\mu\text{L}$  injections given 24 h apart. Mice given a single injection were euthanized at 18, 30, and 48 h after injection. Mice given two injections were euthanized at 42, 48, 54, 72, and 96 h following the initial injection. At each time point, brain, lung, heart, liver, kidney, spleen, tumor, blood, and tail samples were harvested and stored at  $-80$  °C until they could be evaluated for boron content. After several experiments demonstrated minimal boron uptake into the brain, lung, and heart, further analyses of these tissues was discontinued.

Tissues were digested by using a Microwave Accelerated Reaction System (Mars; CEM), and their boron content was determined via inductively coupled plasma optical emission spectroscopy (ICP-OES) with a PerkinElmer Optima 7000 DV in accordance with published methods (44). As a control to determine whether the tail vein injections were successful and therefore whether biodistribution data from a particular animal were valid, tails were routinely analyzed for boron content. Levels of boron in the blood were never observed to exceed 100  $\mu\text{g}$  boron per gram blood; thus, if a tail value exceeded 100  $\mu\text{g}$  boron per gram tail, the injection was assumed to have failed and that animal's data were excluded from the study.

**Therapeutic Effect Studies.** When tumors had reached the 80- to 150- $\text{mm}^3$  target volume, mice were administered  $^{10}\text{B}$ -enriched boronated liposome suspensions via tail-vein injections and subjected to thermal neutron irradiation following the protocol described later. The effect of BNCT was evaluated based on changes in tumor volume over time. Neutron-only tumor-bearing mice were given no boron compounds but were exposed to the same irradiation protocol as the treatment group. Control mice were neither injected with a boron agent nor exposed to thermal neutron irradiation. Tumors on all mice were measured daily with calipers by the same observer throughout the course of an experiment. Measurements were taken until calculated tumor volume exceeded 2,000  $\text{mm}^3$  or the longest diameter exceeded 20 mm. Mice were evaluated daily by a veterinarian or animal care staff for any evidence of ill thrift (failure to thrive) or restricted range of motion.

**Neutron Irradiation.** Just before irradiation, mice were anesthetized by i.p. administration of a combination of 10 mg/kg xylazine and 80 mg/kg ketamine. Cu/Au flux wires were set on the right and left thorax and flank of each mouse before it was placed in a positioning gantry. The gantry held a maximum of four mice or phantoms and permitted selective irradiation of the caudal or cranial half of an animal. To avoid any potential complications and improve the selectivity of the treatment, the head, thorax, and cranial abdomen of the mice were shielded by using  $^6\text{LiCO}_3$  during irradiation. The gantry was placed in the irradiation chamber, and mice were irradiated with thermal neutrons for a maximum of 30 min. A camera in the irradiation chamber permitted observation of animals during treatment. Following irradiation, mice were removed from the gantry and allowed to recover from anesthesia. The Cu/Au flux wires were collected from the mice and counted by using a high-purity germanium  $\gamma$ -spectrometer, and saturation activities were assessed to confirm neutron flux to the animal. The average flux of the neutron beam was determined to be  $8.8 \times 10^8$  neutrons/ $\text{cm}^2\text{-s}$  ( $\pm 7\%$ ) integrated over the (thermal) energy range of 0.0 to 0.414 eV. The measured cadmium ratio for gold was 130:1, indicating contamination with higher energy neutrons was minimal. Thus, for 30 min of irradiation, the approximate background physical doses from hydrogen recoil and nitrogen capture interactions were 41.1 cGy and 34.2 cGy, respectively, and the approximate physical dose from boron capture was 12.9 cGy per 1 ppm of boron in tissue. The incident  $\gamma$ -component of the beam was estimated to be  $\sim 63.6$  cGy, with a small additional  $\gamma$ -component induced by thermal neutron capture in hydrogen. Therefore, assuming a tumor boron concentration of 60 ppm, the physical boron neutron capture dose was  $\sim 7.75$  Gy, well greater than the background components from all sources.

**Data Analysis.** Tumor volumes were calculated by using the equation  $V = \frac{\pi}{6} * l * w * d$ , where  $l$  is the length (greatest longitudinal diameter),  $w$  is the width (greatest transverse diameter), and  $d$  is the diameter (greatest diameter orthogonal to the plane formed by  $l$  and  $w$ ) for an elliptical tumor in millimeters. Time-to-event curves were estimated by using the Kaplan-Meier method (37), and outcomes among treatment groups were compared by using the log-rank test. Biodistribution plots and growth curves were constructed in Microsoft Excel 2007, and survival analysis was conducted by using SigmaPlot 12.0.

**ACKNOWLEDGMENTS.** The authors thank the University of Missouri Research Reactor for providing a thermal neutron beam line, Dr. Cai for collaboration in animal handling and injections, Jonathan Dixon and Melissa Luechtefeld for ICP-OES analysis of tissues, and Pamela Cooper for editing the manuscript. This work was supported by US Department of Energy Grant DE-FG03-95ER61975 and National Institutes of Health Grant R01CA097342.

- Coderre JA, Morris GM (1999) The radiation biology of boron neutron capture therapy. *Radiat Res* 151(1):1–18.
- Hopewell JW, Morris GM, Schwint A, Coderre JA (2011) The radiobiological principles of boron neutron capture therapy: A critical review. *Appl Radiat Isot* 69(12):1756–1759.
- Sweet WH (1997) Early history of development of boron neutron capture therapy of tumors. *J Neurooncol* 33(1-2):19–26.
- Valliant J, et al. (2002) The medicinal chemistry of carboranes. *Coord Chem Rev* 232(1-2):173–230.
- Soloway AH, et al. (1998) The chemistry of neutron capture therapy. *Chem Rev* 98(4):1515–1562.
- Hawthorne M (1993) The role of chemistry in the development of boron neutron capture therapy of cancer. *Angew Chem Int Ed Engl* 32(7):950–984.
- Hawthorne MF (1998) New horizons for therapy based on the boron neutron capture reaction. *Mol Med Today* 4(4):174–181.
- Busse PM, et al. (2003) A critical examination of the results from the Harvard-MIT NCT program phase I clinical trial of neutron capture therapy for intracranial disease. *J Neurooncol* 62(1-2):111–121.
- Diaz AZ (2003) Assessment of the results from the phase III boron neutron capture therapy trials at the Brookhaven National Laboratory from a clinician's point of view. *J Neurooncol* 62(1-2):101–109.
- Barth RF, Coderre JA, Vicente MG, Blue TE (2005) Boron neutron capture therapy of cancer: Current status and future prospects. *Clin Cancer Res* 11(11):3987–4002.
- Henriksson R, et al.; Swedish Brain Tumour Study Group (2008) Boron neutron capture therapy (BNCT) for glioblastoma multiforme: A phase II study evaluating

- a prolonged high-dose of boronophenylalanine (BPA). *Radiother Oncol* 88(2): 183–191.
12. Hopewell JW, et al. (2011) Boron neutron capture therapy for newly diagnosed glioblastoma multiforme: An assessment of clinical potential. *Appl Radiat Isot* 69(12): 1737–1740.
  13. Nakai K, et al. (2011) Boron neutron capture therapy combined with fractionated photon irradiation for glioblastoma: A recursive partitioning analysis of BNCT patients. *Appl Radiat Isot* 69(12):1790–1792.
  14. Kankaanranta L, et al. (2012) Boron neutron capture therapy in the treatment of locally recurrent head-and-neck cancer: Final analysis of a phase III trial. *Int J Radiat Oncol Biol Phys* 82(1):e67–e75.
  15. Hawthorne M, Lee M (2003) A critical assessment of boron target compounds for boron neutron capture therapy. *J Neurooncol* 62(1-2):33–45.
  16. Matsumura Y, Maeda H (1986) A new concept for macromolecular therapeutics in cancer chemotherapy: Mechanism of tumorotropic accumulation of proteins and the antitumor agent smancs. *Cancer Res* 46(12 pt 1):6387–6392.
  17. Fang J, Nakamura H, Maeda H (2011) The EPR effect: Unique features of tumor blood vessels for drug delivery, factors involved, and limitations and augmentation of the effect. *Adv Drug Deliv Rev* 63(3):136–151.
  18. Shelly K, et al. (1992) Model studies directed toward the boron neutron-capture therapy of cancer: Boron delivery to murine tumors with liposomes. *Proc Natl Acad Sci USA* 89(19):9039–9043.
  19. Hawthorne MF, Shelly K (1997) Liposomes as drug delivery vehicles for boron agents. *J Neurooncol* 33(1-2):53–58.
  20. Muetterties E, Balthis J, Chia Y, Knoth W, Miller H (1964) Chemistry of boranes. VIII. Salts and acids of  $B_{10}H_{10}^{2-}$  and  $B_{12}H_{12}^{2-}$ . *Inorg Chem* 3(3):444–451.
  21. Feakes DA, Shelly K, Knobler CB, Hawthorne MF (1994)  $Na_3[B_{20}H_{17}NH_3]$ : Synthesis and liposomal delivery to murine tumors. *Proc Natl Acad Sci USA* 91(8):3029–3033.
  22. Georgiev EM, et al. (1996) Synthesis of amine derivatives of the polyhedral borane anion  $[B_{20}H_{18}]^4-$ . *Inorg Chem* 35(19):5412–5416.
  23. Feakes DA, Waller RC, Hathaway DK, Morton VS (1999) Synthesis and in vivo murine evaluation of  $Na_4[1-(1'-B_{10}H_9)-6-SHB_{10}H_8]$  as a potential agent for boron neutron capture therapy. *Proc Natl Acad Sci USA* 96(11):6406–6410.
  24. McVey WJ, et al. (2008) Investigation of the interactions of polyhedral borane anions with serum albumins. *J Inorg Biochem* 102(4):943–951.
  25. Li F, Shelly K, Knobler CB, Hawthorne MF (1999) The synthesis of  $[Me_4N]_2[a^2-B_{20}H_{16}(NH_3)_2]$  and  $trans-B_{20}H_{16}(NH_3)_2$  from  $[Me_3NH][cis-B_{20}H_{17}NH_3]$  and their structural characterization. *Inorg Chem* 38(22):4926–4927.
  26. Li F, Shelly K, Knobler C, Hawthorne M (1998) A new isomer of the  $[B_{20}H_{18}]^{2-}$  ion: Synthesis, structure, and reactivity of  $cis-[B_{20}H_{18}]^{2-}$  and  $cis-[B_{20}H_{17}NH_3]$ . *Angew Chem Int Ed Engl* 37(13-14):1868–1871.
  27. Hawthorne MF, Shelly K, Li F (2002) The versatile chemistry of the  $[B_{20}H_{18}]^{2-}$  ions: Novel reactions and structural motifs. *Chem Commun (Camb)* 38(6):547–554.
  28. Irani K, et al. (1997) Mitogenic signaling mediated by oxidants in Ras-transformed fibroblasts. *Science* 275(5306):1649–1652.
  29. Oberley TD (2002) Oxidative damage and cancer. *Am J Pathol* 160(2):403–408.
  30. Feakes DA, Shelly K, Hawthorne MF (1995) Selective boron delivery to murine tumors by lipophilic species incorporated in the membranes of unilamellar liposomes. *Proc Natl Acad Sci USA* 92(5):1367–1370.
  31. Straubinger RM, Hong K, Friend DS, Papahadjopoulos D (1983) Endocytosis of liposomes and intracellular fate of encapsulated molecules: Encounter with a low pH compartment after internalization in coated vesicles. *Cell* 32(4):1069–1079.
  32. Straubinger RM, Papahadjopoulos D, Hong KL (1990) Endocytosis and intracellular fate of liposomes using pyranine as a probe. *Biochemistry* 29(20):4929–4939.
  33. Lee KD, Nir S, Papahadjopoulos D (1993) Quantitative analysis of liposome-cell interactions in vitro: Rate constants of binding and endocytosis with suspension and adherent J774 cells and human monocytes. *Biochemistry* 32(3):889–899.
  34. Khalil I, Kogure K, Akita H, Harashima H (2006) Uptake pathways and subsequent intracellular trafficking in nonviral gene delivery. *Pharmacol Rev* 58:32–45.
  35. Heber EM, et al. (2012) Boron delivery with liposomes for boron neutron capture therapy (BNCT): Biodistribution studies in an experimental model of oral cancer demonstrating therapeutic potential. *Radiat Environ Biophys* 51(2):195–204.
  36. Brockman J, Nigg DW, Hawthorne MF, McKibben C (2009) Spectral performance of a composite single-crystal filtered thermal neutron beam for BNCT research at the University of Missouri. *Appl Radiat Isot* 67(7-8, suppl):S222–S225.
  37. Kaplan E, Meier P (1958) Nonparametric estimation from incomplete observations. *J Am Stat Assoc* 53(282):457–481.
  38. Miura M, et al. (2001) Boron neutron capture therapy of a murine mammary carcinoma using a lipophilic carboranyl-tetraphenylporphyrin. *Radiat Res* 155(4):603–610.
  39. Pignol J-P, et al. (1998) Selective delivery of  $^{10}B$  to soft tissue sarcoma using  $^{10}B$ -L-boronophenylalanine for boron neutron capture therapy. *Br J Radiol* 71(843):320–323.
  40. Ono K, et al. (1996) Radiobiological evidence suggesting heterogeneous micro-distribution of boron compounds in tumors: Its relation to quiescent cell population and tumor cure in neutron capture therapy. *Int J Radiat Oncol Biol Phys* 34(5): 1081–1086.
  41. Twentyman PR, Bleeher NM (1976) The sensitivity to cytotoxic agents of the EMT6 tumor in vivo. Comparative response of lung nodules in rapid exponential growth and of the solid flank tumour. *Br J Cancer* 33(3):320–328.
  42. Kwok TT, Twentyman PR (1985) The response to cytotoxic drugs of EMT6 cells treated either as intact or disaggregated spheroids. *Br J Cancer* 51(2):211–218.
  43. Kreimann EL, et al. (2001) The hamster cheek pouch as a model of oral cancer for boron neutron capture therapy studies: Selective delivery of boron by boronophenylalanine. *Cancer Res* 61(24):8775–8781.
  44. Sun D-H, Waters J, Mawhinney T (1997) Microwave digestion and ultrasonic nebulization for determination of boron in animal tissues by inductively coupled plasma atomic emission spectrometry with internal standardization and addition of mannitol. *J Anal At Spectrom* 12(6):675–679.